

# Gravity wave influence on middle atmosphere dynamics in model and satellite data

P. Hoffmann, Ch. Jacobi

## Abstract

Numerical results of the Middle and Upper Atmosphere Model (MUAM) for simulating the middle atmosphere conditions during January-February 2006 and 2008 have been compared with SABER/TIMED satellite data. A weaker amplitude of stationary waves in the mesosphere was found in 2008 compared to 2006. By forcing the model with realistic lower boundary conditions from reanalyses, averaged fields of zonal wind and temperature as well as stationary waves were simulated. Through changing of gravity wave (GW) amplitudes in the parameterisation, such a realistic behaviour can be approximately reproduced with model. We conclude that at least part of the middle atmosphere interannual variability is due to changes in GW forcing.

## 1. Introduction

Mechanistic circulation models of the middle atmosphere include simplified numerical schemes of some dynamical processes such as the gravity wave (GW) interaction with the mean flow. Their application is limited and parts of the input parameters, such as GW sources and the distribution of ozone, only consider zonal symmetric structures. In some models essentially tuned to describe the middle atmosphere like the Middle and Upper Atmosphere Model (MUAM, Pogoreltsev et al., 2007), the scheme that characterises the acceleration of the mean wind due to GW is insufficient to study coupling processes with the thermosphere, because the parameterisation only describes slowly GW with a fixed horizontal wavelength of 300 km, which cannot penetrate the lower thermosphere. Nevertheless, middle atmosphere processes may be approximately reproduced by the model. In this paper we compare two model runs for Jan-Feb 2006 and 2008 with satellite data. In other words, we are interested in how MUAM is able to reproduce the two different observations by simply changing the lower boundary conditions and the amplitude of GW. Figure 1 shows results from satellite data analysis at 45°N, that is the distribution of stationary planetary waves (SPWs) with height over the time from 2002 to 2008. A wave proxy is used based on standard deviations of temperatures from the SABER/TIMED instrument (Mertens and et al., 2001, 2004); a description of this proxy can be found in Hoffmann and Jacobi (2010); Borries and Hoffmann (2010). While in winter (Jan-Feb) 2006 the amplitudes of the mesospheric stationary wave component is well developed, two years later there exists almost no signal of SPW. It is supposed that such behaviour may be indirectly connected with the solar cycle that influences the dynamics of the middle atmosphere. Data analyses of GW potential energy also derived from SABER temperature profiles (Jacobi et al., 2011) of the last years have shown an increase of the mean GW activity in the mesosphere, which might be interpreted for this hypothesis. However, in contrast to the situation in summer, winter conditions are mainly affected by PW activity. GWs play the most important role. Thus, Fig. 2 presents global Jan-Feb mean GW potential energy and its change during the period from 2006 to 2008. Positive

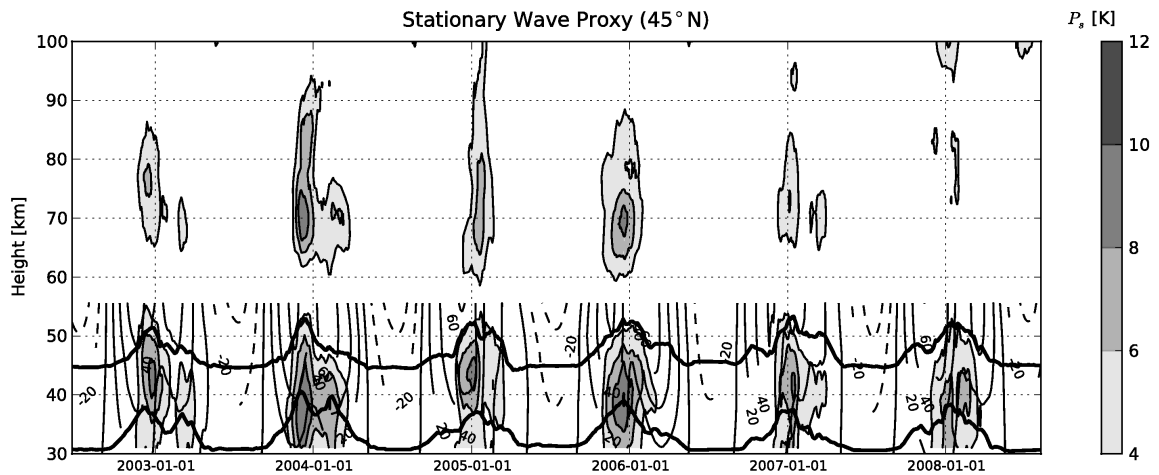


Figure 1: *Height-time cross section of a wave proxy derived from SABER temperatures at 45°N (grey scaling) from 2002-2008. The mean zonal wind (grey contours) and the same proxy at 30 km and 45 km (heavy black lines) obtained by MetO are added.*

deviations (middle panel of Fig. 2) in the upper mesosphere (~80 km) denote stronger GW activity in 2006 than in 2008. An opposite sign is found in the lower thermosphere, which means a decrease of GW energy between the two years. Although the comparison of GW for these individual years indicates deviations from the current long-term trend the downward shifting of the breaking level (~90 km) with increasing GW can be seen that motivates us for this comparison study.

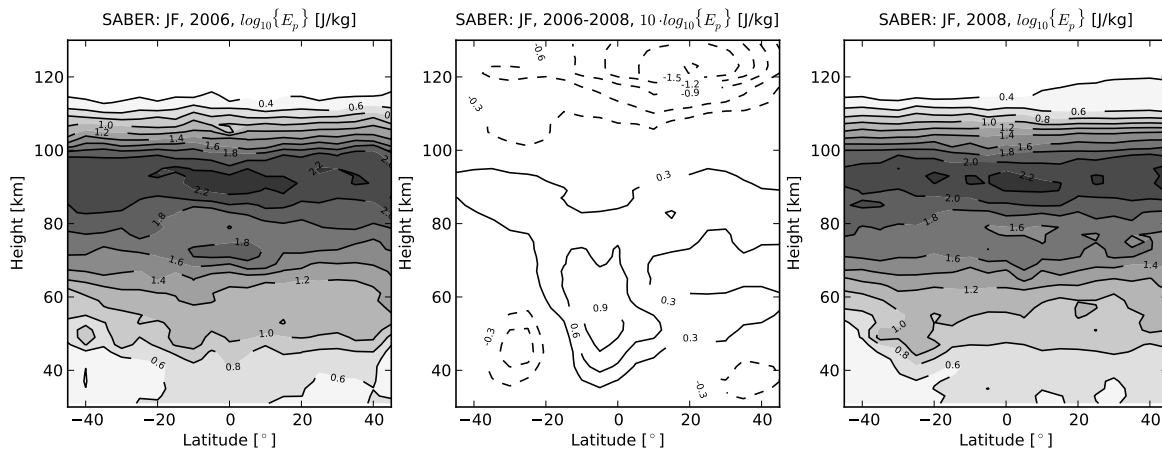


Figure 2: *Height-latitude cross section of Jan-Feb (JF) mean zonal averaged GW potential energy ( $E_p$ ) for 2006 (left panel) and 2008 (right panel). The 2006-2008 difference pattern is shown in the middle of this figure. Note that the difference values are multiplied by factor of 10.*

In order to simulate the response of middle atmosphere dynamics on GW changes we amplify their amplitude to simulate changes in the middle atmosphere that are in accordance with SABER results and compare the different model results for the mean flow with satellite observations. For that purpose, global data from MetOffice stratospheric reanalyses

(MetO, Swinbank and Ortland, 2003) and unevenly spaced temperature profiles of the stratosphere, mesosphere and lower thermosphere provided by the SABER instrument are analysed with respect to planetary waves (PW) for comparison with the model. The following sections will give a coarse introduction to the circulation model (MUAM) and satellite data (SABER/TIMED) as well as the space-time method for analysing PW.

## 2. The middle and upper atmosphere model (MUAM)

The MUAM model (Pogoreltsev et al., 2007) was developed on the basis of the Cologne Model of the Middle Atmosphere-Leipzig Institute for Meteorology (COMMA-LIM), which was already applied in previous studies, e.g., by Fröhlich et al. (2003b); Jacobi et al. (2006). It is a so-called mechanistic three-dimensional model, in which the atmosphere circulation is self-consistently generated. Monthly zonal means of the geopotential height and temperature fields, that cover the troposphere and lower stratosphere up to 10 hPa, as well as the monthly averaged amplitude and phase of the first three zonal harmonics at 1000 hPa, taken from reanalysis data, are used as lower boundary conditions. These are typically averaged over 10 years (1992-2002). The radiative heating due to absorption  $O_3$  and  $O_2$  is described in the Strobel-scheme (Strobel, 1978) and the heating of  $H_2O$  and  $CO_2$  is adjusted according to (Liou, 1992). The effect of GW on the circulation in the model is parametrised by a scheme based on Lindzen (1981).

The breaking of GW occurs, if the static stability vanishes, which corresponds to  $\partial\theta/\partial z = 0$ , and causes turbulence, mixing and GW dissipation in the upper mesosphere. Other modifications in this scheme has been implemented by Jacobi et al. (2006) as proposed in Gavrilov and Yudin (1992); Gavrilov and Fukao (1999); Akmaev (2001). A detailed description of the implemented parameterisations can be found in Fröhlich et al. (2003a). Several studies of planetary waves propagation in the middle atmosphere using COMMA-LIM were made by, e.g., Fröhlich et al. (2003b, 2005); Jacobi et al. (2006).

The 60-level version of MUAM allows to include the dynamics of the neutral upper atmosphere (thermosphere) by shifting the upper boundary to a height of about 300 km and incorporating a new scheme for extreme ultra-violet (EUV) heating based on the work of Richards et al. (1994). The 48-level version only considers the middle atmosphere up to about 135 km. The horizontal resolution in latitude and longitude is  $5^\circ \times 5.625^\circ$  and the vertical levels are given by the non-dimensional height  $x = -\ln(p/1000 \text{ hPa})$ . The log-pressure height is obtained by multiplying  $x$  the non-dimensional height with the scale height ( $H = 7 \text{ km}$ ).

Description	Symbol	Values	Unit
number of gravity waves		48	
horizont. wavelength	$\lambda_x$	300	km
phase speed	$c_i$	5, 10, 15, 20, 25, 30	m/s
azimuth angle	$\theta$	0, 45, 90, 135, 180, 225, 270, 315	deg

Table 4: Overview about parameters, which determine the spectrum of typical GW as used in the parametrisation scheme of MUAM.

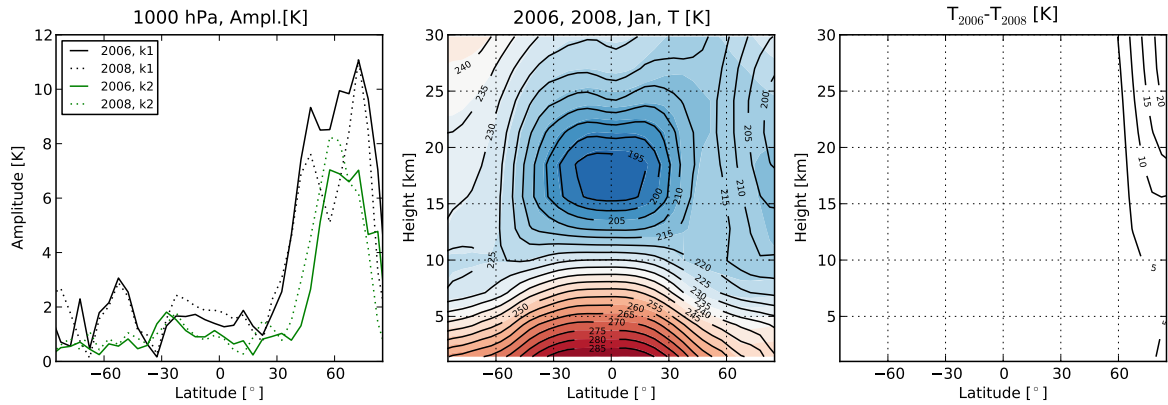


Figure 3: Lower boundary for January condition of the years 2006 and 2008 that are used in the model runs as a function of latitude and/or height: temperature amplitude distribution for zonal wavenumbers  $k=1,2$  at 1000 hPa (left panel), mean temperature cross sections (mid panel) and the difference (right panel).

Here, the 48-level version of MUAM is applied in order to study the effect of GW changes on the middle atmosphere dynamics. In Tab. 4 parameters are listed, which indicate the spectrum of GW as considered in the parametrisation. Altogether 48 different kinds of GW are characterised by typical values of phase speed, horizontal wavelength and azimuth angle, which are implemented in 10 km. Their vertical velocity is weighted by frequency and phase speed as described in Jacobi et al. (2006). Latitudinal and seasonal dependencies are also considered in the parameterisation. Though, a stronger GW activity in the winter hemisphere is supposed.

### 3. Reanalyses and satellite data

Operational reanalyses from MetOffice (Swinbank and Ortland, 2003) and measurements from the SABER instrument on board of the TIMED satellite (Mlynczak, 1997) are analysed here in order to evaluate the model results. While the standard reanalysis products of meteorological parameters are provided on a regular grid up to the lower mesosphere ( $\sim 60$  km), additional information of the temperature distribution in the stratosphere, mesosphere and lower thermosphere (30-130 km) can be retrieved from satellite (Mertens and et al., 2001, 2004). These data are unevenly spaced according to the orbital geometry. By applying spectral methods (Section 4) harmonic components are extracted from the data and compared with model results.

#### 3.1 Boundary conditions to run the model

For running MUAM for two different Jan-Feb conditions in 2006 and 2008, the monthly mean zonal averaged temperature field up to 30 km and the first three stationary components at 1000 hPa with zonal wavenumber  $k=1,2,3$  in temperature and geopotential height are extracted from NCEP/NCAR reanalyses (Kalnay et al., 1996) and implemented as lower boundary condition.

Figure 3 shows parts of the used lower boundary conditions to setup the model to situations that correspond to Jan 2006 and Jan 2008. The middle panel presents the monthly

zonal mean temperature pattern in the height-latitude cross section. The difference pattern between Jan 2006 and Jan 2008 is shown in the right panel and indicates a 10 K warmer lower north polar stratosphere in 2006. The monthly mean amplitudes of the first two harmonics (left panel), which corresponds to stationary planetary waves SPW1 (black) and SPW2 (green), reveal differences between 2006 (solid) and 2008 (dashed) at the lowest pressure level (1000 hPa). In particular, the SPW1 amplitudes at midlatitudes differ by about 2 K.

### 3.2 Satellite data analysis

The stratosphere, mesosphere and lower thermosphere satellite-based remote sensing techniques products (e.g. TIMED/SABER) extend the data base provided by reanalyses. In particular, limb-sounding of temperature profiles (Mertens and et al., 2001, 2004) provide useful information about the thermal structure and composition between the height-latitude range of 30-130 km and from 52° to 83° on the other hemisphere. After a 60 days yaw-cycle the latitude range reverses. Thus, since the instrument starts its observations in January 2002, a nearly continuous temperature coverage is available in a latitude range of about 50°S to 50°N.

For analysing the unevenly spaced data, taken from the so-called L2A (V1.07) product, with respect to PW we separated temperature into ascending ( $T_{asc}$ ) and descending ( $T_{dsc}$ ) nodes (Oberheide et al., 2003) and arranged the daily orbital information to a regular 3D-grid  $[\Delta z, \Delta \phi, \Delta \lambda] = [2 \text{ km}, 5^\circ, 10^\circ]$  covering the middle atmosphere from  $\phi = [-45^\circ \dots 45^\circ]$  and  $z = [30 \dots 130 \text{ km}]$ . By collecting all temperature values within such a grid box and averaging, a data set for analysing PW in the stratosphere and mesosphere is obtained. In the upper mesosphere and lower thermosphere, tidal effects blur a clear picture of PW. Spectral methods for analysing unevenly spaced data in the longitude and time domain (e.g. Hayashi, 1980; Zhang et al., 2006; Pancheva et al., 2009a,b) is applied to decompose PW and tides from polar orbiting satellite data in one step.

## 4. Analysis of waves

For the analysis of mean fields and wave components with respect to wavenumber ( $k$ ) and frequency ( $\omega$ ) from unevenly spaced satellite data the method introduced in Pancheva et al. (2009a) is applied. This method also allows to analyse evenly spaced reanalyses and model output data. Based on a two-month data set (Jan-Feb) the algorithm is adopted for each height and latitude separately, in order to obtain a global characteristic of PW activity. For each analysis, all longitudinal and temporal information  $X_{\phi,z}(t, \lambda)$  are arranged in one vector and decomposed into mean ( $A_m$ ), higher order trends ( $A_t, A_p$ ) and harmonic components as given next:

$$\begin{aligned}
X(t, \lambda) &= A_m + A_t \cdot t + A_p \cdot t^2 \\
&+ \sum_{n=1}^{16} A_v \cdot \cos(\omega_n t + \varphi_v) \\
&+ \sum_{k=1}^{16} A_s \cdot \cos(k\lambda + \varphi_s) \\
&+ \sum_{n=1}^{16} \sum_{k=0}^3 A_w \cdot \cos(k\lambda + \omega_n t + \varphi_w) \\
&+ \sum_{n=1}^{16} \sum_{k=0}^3 A_e \cdot \cos(k\lambda - \omega_n t + \varphi_e) \\
&+ R(t, \lambda).
\end{aligned} \tag{1}$$

A least-squares (LS) method is then applied to determine the extracted spectral wave characteristics with respect to frequencies ( $\omega_n$ ) and zonal wavenumbers ( $k$ ) for the amplitude and phase of vacillations ( $A_v, \varphi_v$ ), stationary waves ( $A_s, \varphi_s$ ) and westward ( $A_w, \varphi_w$ ) and eastward travelling waves ( $A_e, \varphi_e$ ).  $R$  gives the residual between analysis model and data. Here, we use this method to exclusively decompose the unevenly spaced SABER temperature profiles into the mean and stationary wave components. Alternatively, we compute proxies of travelling ( $P_t$ ) and stationary ( $P_s$ ) waves (Hoffmann and Jacobi, 2010) to compare planetary wave activity between different model runs.

## 5. Model comparison with data in the winters 2006 and 2008

In this section we present differences between model results for winter conditions (Jan-Feb) of the years 2006 and 2008 in comparison with SABER data. In order to run the model for these two cases, the lower boundary conditions of January 2006 and 2008 were extracted from NCEP reanalysis to replace the climatological data for 1992-2002 (see section 3.1). All runs were carried out without externally forced travelling PW. However, free travelling internal waves are self-consistently generated by the model. There are additional parameters (e.g. the amplitude of GW at the equator) that are adapted to the respective situations.

MUAM runs	year (lower boundary)	GW	figures
1	2006	2.0 cm/s	6, 7, 8, 9
2	2008	2.0 cm/s	6, 7, 8, 9, 11, 12
3	2008	2.2 cm/s	11, 12

Table 7: *List of model runs (330-390 days) and figures that demonstrate our results.*

At first we run the model by using the two different initial data. All other adjustments are equal (see Tab. 7). Although the lower boundaries represent January conditions, the model simulates January and February fields (model day 330-390). The period of time between model day 300 to day 330 corresponds to January 1 conditions over one month.

After that the seasonal variation of the sun begins. All used monthly mean climatological datasets, e.g., the distribution of ozone, represent still January condition. Next, another run is carried out by slightly increasing the GW amplitude from 2.0 to 2.2 cm/s (*run3*). Since the last solar maximum ( $\sim 2002$ ) an increasing of GW activity in the mesosphere is observed, e.g., by analysing GW potential energy from SABER temperature profiles, which motivates runs with modifies GW amplitudes.

### 5.1 Synoptic interpretation

Figure 1 shows a strong decrease of the SPW in the mesosphere at  $45^\circ\text{N}$  from 2006 to 2008. In order to investigate possible reasons for that we consider the two winter situations in more detail.

In the following Fig. 4 presents the mean zonal wind (contours) and temperature anomalies (color scaling) at  $45^\circ\text{N}$  obtained by MetO (lower panels) and SABER (upper panels). The time interval ranges from October 1 to March 31, respectively. The SABER data used here are daily values regridded on an evenly spaced 3-dimensional structure and the geostrophic approximation is applied to derive the zonal wind component from the horizontal pressure gradient. The values above 80 km should be regarded with care due to the tidal signals, which are not removed from the data.

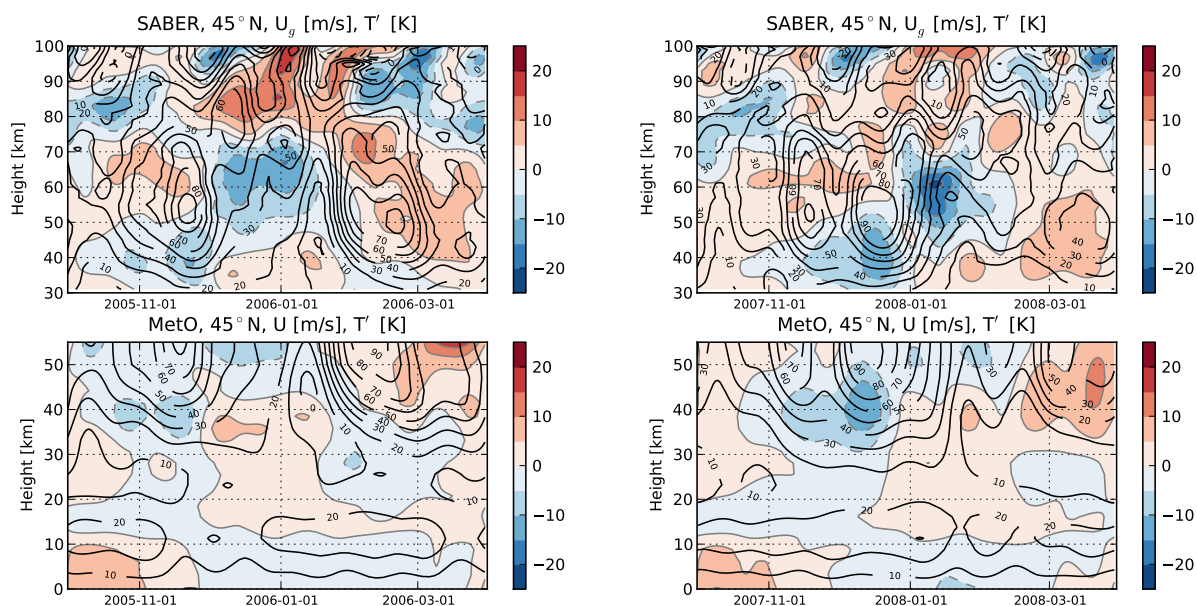


Figure 4: *Height-time cross section of smoothed zonal wind (contours) and temperature anomalies (color scaling) taken from MetO (lower panels) and SABER (upper panels) between the 1st October to 31st March of 2006 (left) and 2008 (right) at  $45^\circ\text{N}$ .*

The temporal behaviour in wind and temperature anomalies within the corresponding height range (30-55 km) is similar in the absolute values and the location of the jets. Both cases indicate a warming in the stratosphere (+5 K) connected with cooling in the mesosphere (-10 K) around Dec-Jan 2006 and Jan-Feb 2008. Before the temperature increase occurs, the zonal wind is strong, but much weaker during the warming period. A complete wind reversal, known from sudden stratospheric warming (SSW), is not observed

because this phenomenon is primarily located at higher latitudes (e.g. Labitzke, 1999; Hoffmann et al., 2007).

Figure 5 shows height-latitude patterns of Jan-Feb mean field differences between 2006 and 2008 of SABER temperature (left panel) and the amplitude of SPW1 (right panel). From mean temperature deviations, we may see that the summer hemisphere is hardly affected and the differences are weak. The equatorial region and winter hemisphere indicate a change of positive and negative anomalies, while positive signs correspond to larger values in 2006. Accordingly, a cooling of the tropical mesosphere (50-70 km) is observed, which is accompanied by a warming at midlatitudes. The upper mesosphere (>70 km) shows an opposite behaviour, that is a cooling at 45°N. Considering the change in SPW activity between 2006 and 2008, a decreasing amplitude of more than 2 K is observed in the mesosphere  $\sim$ 70 km, as already depicted in Fig. 1.

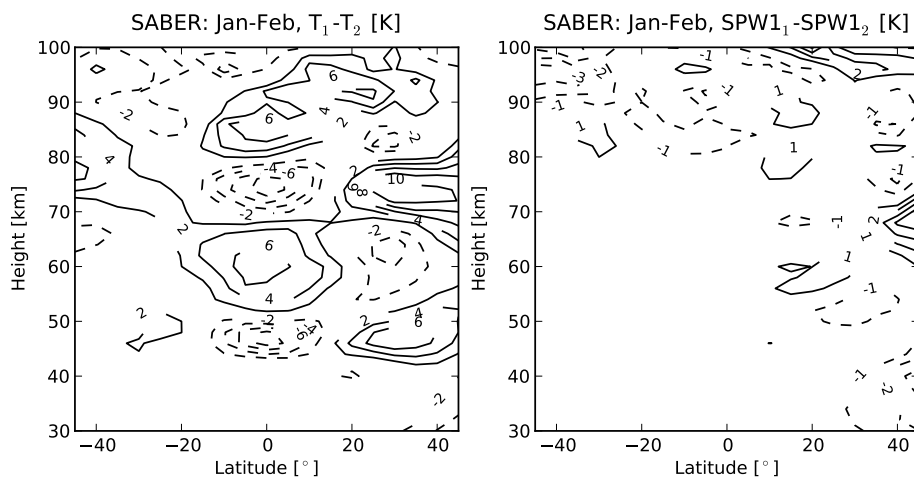


Figure 5: Height-latitude pattern of 2006-2008 differences of Jan-Feb mean temperature (left panel), and stationary waves (right panel).

## 5.2 Modelled differences by changing the lower boundary conditions

In this subsection we compare Jan-Feb mean zonal wind and temperature fields in the middle atmosphere obtained by model simulations (color scaling) with MetO (contours). The following figures show the individual two-monthly mean distributions in height-latitude cross sections of the year 2006 (left) and 2008 (right) as well as the deviations between the two patterns (middle).

Figure 6 compares the 2006 and 2008 mean zonal winds in Jan-Feb. Both model simulations (*run1*, *run2*) represent the known characteristics of the westerly and easterly jets in the middle atmosphere. The height level of the wind reversal in the mesopause region depends on the GW amplitude. In the two considered cases this parameter is set to 2 cm/s at the equator. The comparison between model and reanalyses up to about 55 km reveals a qualitatively better agreement for the summer than for the winter hemisphere. The reason is that no PW are able to exist during easterly winds. In contrast, on the winter hemisphere the mean wind is influenced by waves, which makes it more complicated to reproduce data by model simulations without externally forced travelling PW. For this reason one can sometimes reproduce observations very well (e.g. 2006) and sometimes less satisfactorily (2008).

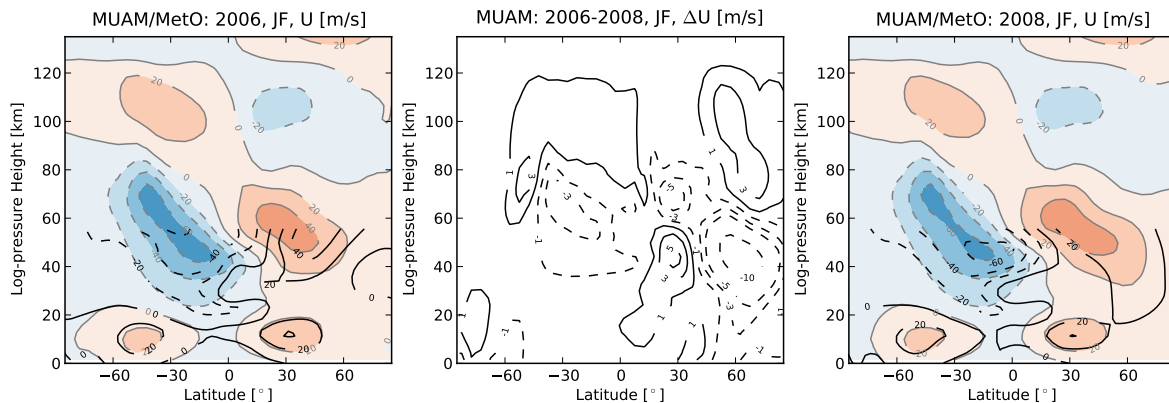


Figure 6: *Height-latitude cross section of mean zonal wind for Jan-Feb 2006 (left panel) and 2008 (right panel) generated by MUAM (colour code). MetO zonal winds are overlayed as isolines. The difference pattern is shown in the middle panel.*

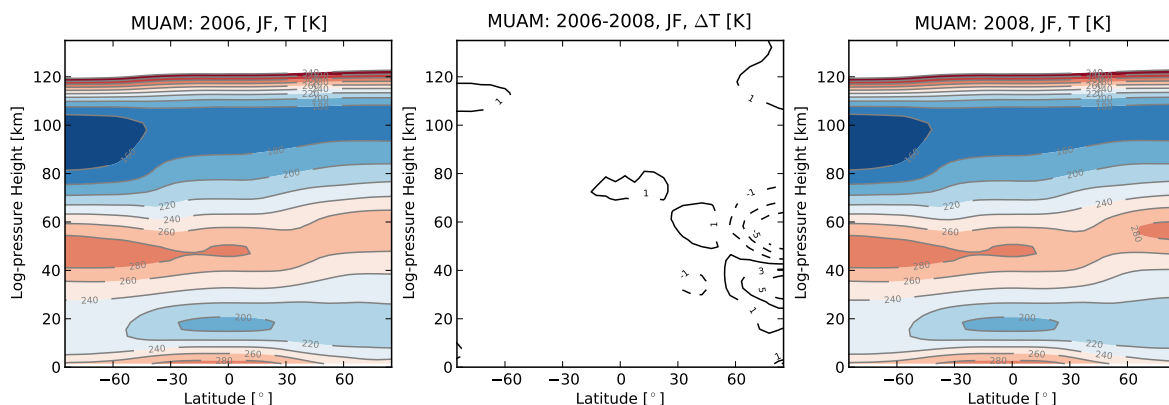


Figure 7: *Height-latitude cross section of mean temperature for Jan-Feb 2006 (left panel) and 2008 (right panel) generated by MUAM. The difference pattern is shown in the middle panel.*

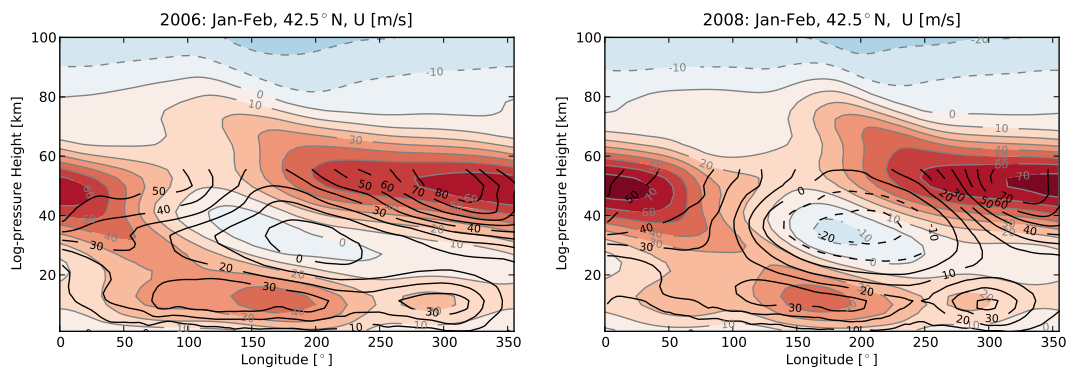


Figure 8: *Height-longitude cross section of zonal wind at 42.5°N modelled by MUAM (color scaling) and MetO (contours).*

Regarding the differences between the same two model simulations (*run1* and *run2*), Fig. 6 (middle panel) reveals negative (dashed lines) and positive (solid lines) anomalies in the zonal wind. Negative anomalies prevail in the region of the middle atmosphere jets, which mean generally stronger westerly winds in 2008 than in 2006 only due to changes of the lower boundary conditions.

Figure 7 presents the temperature distribution of the middle atmosphere for the same cases. The difference of the two patterns reveals a cooling (+5 K) of the stratosphere in 2008 and warming (-5 K) of the mesosphere at high latitudes in 2006. This behaviour can be explained by PW activity. Because externally forced travelling PW are not excited here, differences in SPW activity generated by the lower boundary must be responsible, which is discussed in the following paragraph.

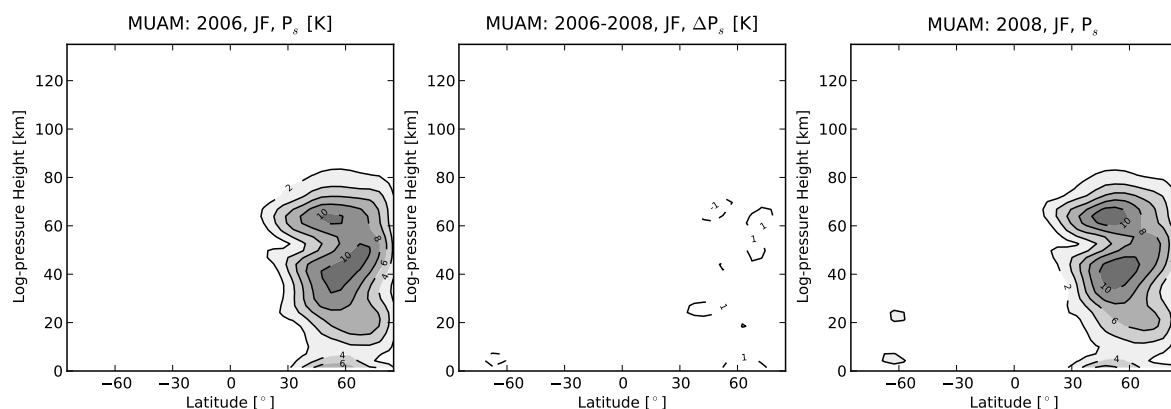


Figure 9: *Height-latitude cross section of the stationary wave proxy in temperature for Jan-Feb 2006 (left panel) and 2008 (right panel) generated by MUAM. The difference pattern is shown in the middle panel.*

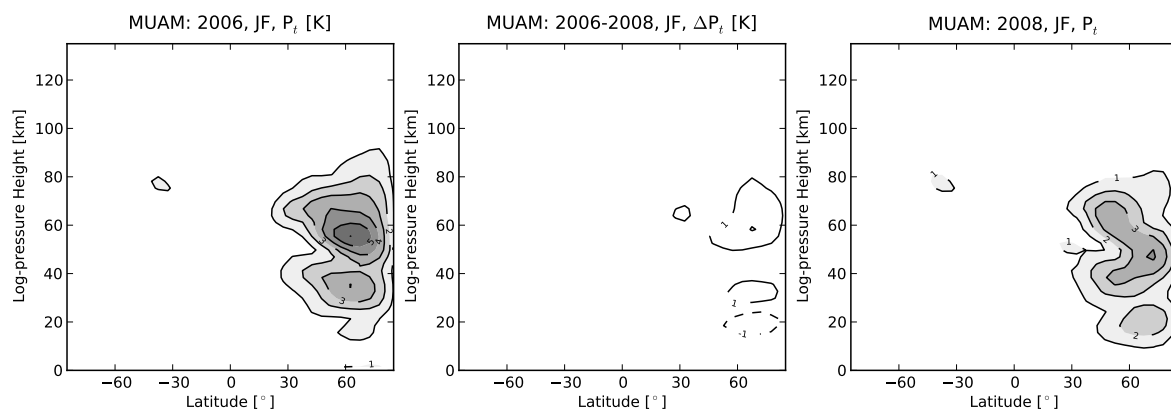


Figure 10: *Height-latitude cross section of the travelling wave proxy in temperature for Jan-Feb 2006 (left panel) and 2008 (right panel) generated by MUAM. The difference pattern is shown in the middle panel.*

It is known that most of the variations caused by PW occur in winter during which westerly winds prevail. Accordingly, we consider the mean zonal wind pattern in the

height-longitude plane at 42.5°N. Figure 8 presents again the two winter situations of 2006 (left part) and 2008 (right part) comparing MUAM (color scaling) and MetO (contours). In 2008 negative values of the zonal wind in the stratosphere over 150°E and 250°E can be observed in both data sets. However, these are stronger in MetO (-20 m/s) than in MUAM data (-10 m/s). In 2006 all values are positive (westerly). The strongest westerly winds with 70 m/s are observed over the Atlantic ocean (300°E to 0°E) in the lower mesosphere in 2008. From Fig. 5 one can estimate the magnitude of the stationary wave 1 in zonal wind to about 30-40 m/s between 50-60 km.

SPW are mainly forced in the troposphere. The amplitude of SPW1 at 1000 hPa may reach 10 K in the winter hemisphere (see Fig. 3). Here, we only consider proxies of stationary waves ( $P_s$ ). In order to obtain the distribution shown in Fig. 9, we calculate the time mean of an 4-dimensional array that includes temperature data arranged in longitude, latitude, altitude and time. Then the standard deviations w.r.t the longitudes are computed. The outer two panels in Fig. 9 show small differences the standard deviation between the two model runs for 2006 and 2008. From SABER data long-term analysis it is expected that the secondary maximum of the SPW proxy in the mesosphere almost vanishes at midlatitudes. This is not the case comparing *run1* with *run2*.

The travelling PW proxy component is shown in Fig. 10. This proxy mainly represents atmospheric normal modes, for which it is assumed that the source is noise in the meteorological parameters in the troposphere or nonlinear interaction between SPW and the mean flow (e.g. Pogoreltsev et al., 2007).

#### 5.4 Model differences by changing of gravity wave amplitudes

One major uncertainty in numerical models is caused by the parameterisation of small scale processes such as GWs. In Fig. 9 it could be shown that without changes of GW amplitudes one cannot reproduce seasonal or year-to-year variability. Thus, a third model run (*run3*) has been carried out with increased GW amplitudes. One expects in such a case that the breaking level and the zonal mean wind reversal descends.

Figure 11 depicts the acceleration rate (ACC) of the mean zonal wind due to GW for the two situations. A larger amplitude of GW in 2008 (*run3*) leads to a stronger deceleration of the mean flow in the upper mesosphere. We interpret the positive anomalies between 2006 and 2008 in the winter hemisphere around 70 km as a stronger deceleration rate of about 1 m/s/d. The effects in the southern hemisphere are more pronounced.

Recently, analyses of GW potential energy derived from SABER temperature profiles (Jacobi et al., 2011) have shown that the GW activity from 2003 to 2008 is increasing in the mesosphere. Above, in the lower thermosphere a decrease is observed.

The model results using the different amplitudes of GW for Jan-Feb conditions in 2008 are shown in Fig. 12. These patterns obtained by MUAM reveal similarities to the patterns in Fig. 5 obtained by SABER. At first we consider the temperature anomalies. In both the observation and model data one can find negative values at about 40 km over the tropics and positive values around 60 km altitude. At low latitudes (20°N-40°N) of the northern hemisphere one can readoff positive deviations around 40 km (+1 K) and stronger negative values at about 60 km (-5 K), which indicates a warming of the stratosphere. In contrast, the mesosphere is cooling during the two years by +3 K (MUAM) and +10 K (SABER). Note that positive differences represent cooling from 2006 through 2008.

The similar behaviour shows the comparison of SPW between model and data reveals

promising results. Although we use different methods for analysing stationary components, for SABER (one-step) and MUAM (proxies), a positive deviation around  $40^{\circ}\text{N}$  and 70 km is observed in model (*run3*) and SABER analyses. A positive anomaly implicates a stronger secondary maximum in 2006 than in 2008 (about 2-3 K). Due to the stronger GW amplitudes the wind reversal in the mesopause region descends and causes a damping of the SPW in the mesosphere. Figure 12 (left panel) confirms this change in the middle atmosphere circulation by a drop of the westerly jet on the winter hemisphere of about 15 m/s at low-latitudes and at 70 km log-pressure height.

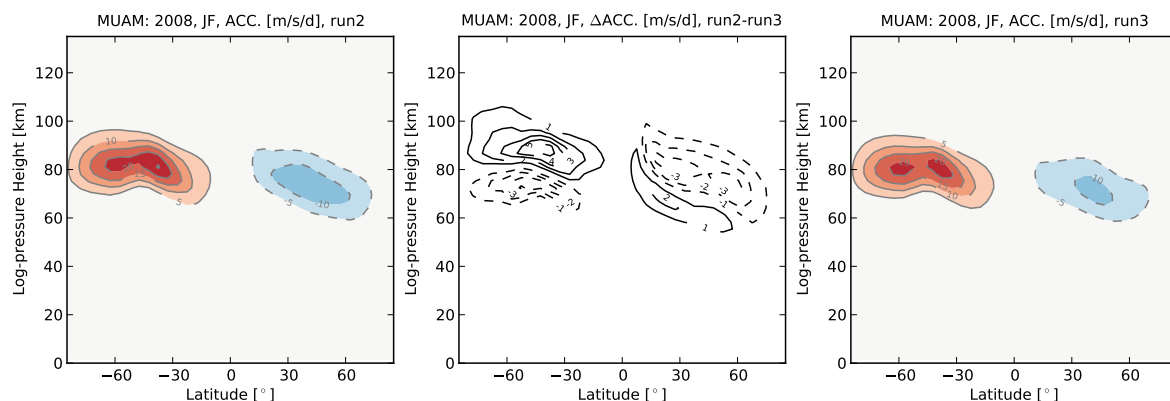


Figure 11: *Height-latitude cross section of acceleration rates for the zonal direction in Jan-Feb 2006 (left panel) and 2008 (right panel) generated by MUAM. The difference pattern is shown in the middle panel.*

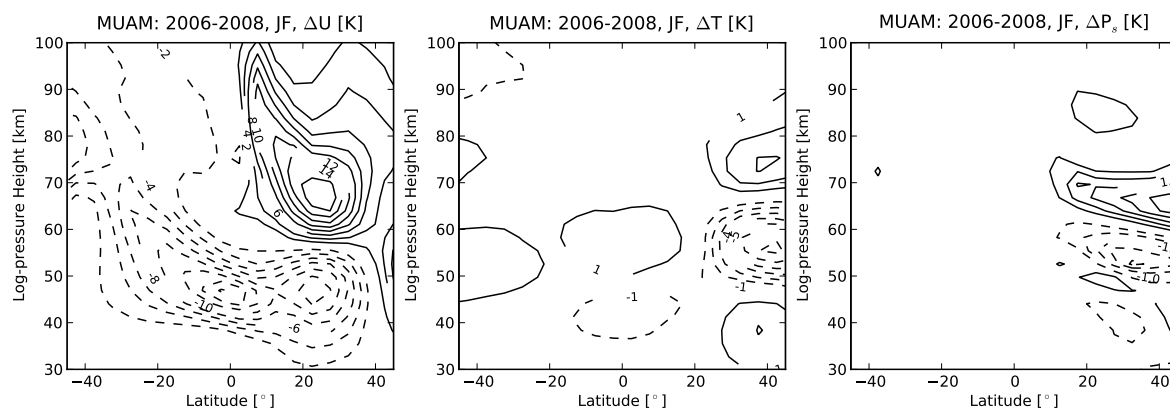


Figure 12: *Height-latitude cross section of differences between model run2 and run3 of mean zonal wind (left panel), temperature (middle panel) and stationary wave proxy (right panel).*

## 6. Conclusions

A mechanistic model of the middle and upper atmosphere has been applied in order to estimate the differences between two winters. The results has been compared with

observations. Until now such models are mainly used to study processes in middle atmosphere dynamics on the basis of climatological (long-term mean) lower boundary conditions. Here, model sensitivity studies have been carried out with monthly mean reanalyses data of January 2006 and 2008 to simulate individual seasons. For comparison satellite temperature data from the SABER instrument (30-130 km) and MetO reanalyses (0-55 km) were used.

It was shown by two examples for Jan-Feb 2006 and 2008 that current model runs cannot reproduce the observations by only changing the lower boundary mean fields. However, it has been demonstrated that the secondary SPW maximum in the lower mesosphere is reduced by increasing GW amplitudes. This is in accordance with SABER observations in 2008.

From these simulations we conclude that mechanistic models like MUAM require a detailed climatology of GW activity dependent on year, season, latitude, and height. A longitudinal distribution may also help in this context. Thus, the analysis of GW energy from satellite temperature profiles up to 130 km (Hoffmann and Jacobi, 2010) would be suitable to install such a climatological database in the model.

## Acknowledgments

This study was supported by Deutsche Forschungsgemeinschaft under grant JA 836/24-1. Many thanks to the British Atmospheric Data Centre (BADC) for providing the MetOffice reanalyses and to NASA for providing the SABER/TIMED satellite measurements. Special thanks to Ekaterina Suvorova and Alexander Pogoreltsev (RSU) for technical advises for running the MUAM model.

## References

- Akmaev, R. A. (2001). Simulation of large scale dynamics in the mesosphere and lower thermosphere with Doppler-spread parameterization of gravity waves. 2. Eddy mixing and the Diurnal Tide. *J. Geophys. Res.*, 102:1203–1205.
- Borries, C. and Hoffmann, P. (2010). Characteristics of F2-layer planetary wave-type oscillations in northern middle and high latitudes during 2002 to 2008. *J. Geophys. Res.*, 115:A00G10, doi:10.1029/2010JA015456.
- Fröhlich, K., Jacobi, C., and Pogoreltsev, A. I. (2005). Planetary wave transience effects on the zonal mean flow: simulations with the COMMA-LIM model. *Adv. Space Res.*, 35:1900–1904.
- Fröhlich, K., Pogoreltsev, A., and Jacobi, C. (2003a). The 48-layer comma-lim model: Model description, new aspects and climatology. *Rep. Inst. Meteorol. Uni. Leipzig*, 30:149–155.
- Fröhlich, K., Pogoreltsev, A. I., and Jacobi, C. (2003b). Numerical simulation of tides, Rossby and Kelvin waves with the COMMA-LIM model. *Adv. Space Res.*, 32:863–868.
- Gavrilov, N. M. and Fukao, S. (1999). A comparison of seasonal variations of gravity wave intensity observed with the middle and upper atmosphere radar with a theoretical model. *J. Atmos. Sci.*, 56:3485–3494.

- Gavrilov, N. M. and Yudin, V. A. (1992). Model for coefficients of turbulence and effective Prandtl Number produced by breaking gravity waves in the upper atmosphere. *J. Geophys. Res.*, 97:7619–7624.
- Hayashi, Y. (1980). A method for estimating space-time spectra from polar-orbiting satellite data. *J. Atmos. Sci.*, 37:1385–1392.
- Hoffmann, P. and Jacobi, C. (2010). Connection of planetary waves in the stratosphere and ionosphere by the modulation of gravity waves. *Rep. Inst. Meteorol. Univ. Leipzig*, 47:23–36.
- Hoffmann, P., Singer, W., Keuer, D., Hocking, W. K., Kunze, M., and Murayama, Y. (2007). Latitudinal and longitudinal variability of mesospheric winds and temperatures during stratospheric warming events. *J. Atmos. Solar-Terr. Phys.*, 69:2355–2366.
- Jacobi, C., Fröhlich, K., and Pogoreltsev, A. I. (2006). Quasi two-day-wave modulation of gravity wave flux and consequences for planetary wave propagation in a simple circulation model. *J. Atmos. Solar-Terr. Phys.*, 68:283–292.
- Jacobi, C., Hoffmann, P., Placke, M., and Stober, G. (2011). Some anomalies of mesosphere/lower thermosphere parameters during the recent solar minimum. *Adv. Radio Sci.*, accepted.
- Kalnay, E., Kanamitsu, M., Kistler, R., Collins, W., Deaven, D., Gandin, L., Iredell, M., Saha, S., White, G., Woollen, J., Zhu, Y., Leetmaa, A., Reynolds, R., Chelliah, M., Ebisuzaki, W., Higgins, W., Janowiak, J., Mo, K. C., Ropelewski, C., and Wang, J. (1996). The NCEP/NCAR 40-year reanalysis project. *Bull. Amer. Meteor. Soc.*, 77:437–470.
- Labitzke, K. (1999). *Die Stratosphäre*. Springer Verlag.
- Lindzen, R. S. (1981). Turbulence and stress owing to gravity waves and tidal breakdown. *J. Geophys. Res.*, 86:9709–9714.
- Liou, K. N. (1992). *Radiation and Cloud Processes in the Atmosphere*, page 487. Oxford Monographs on Geology and Geophysics.
- Mertens, C. J. and et al. (2001). Retrieval of mesospheric and lower thermospheric kinetic temperature from measurements of CO<sub>2</sub> 15 mm earth limb emission under non-LTE conditions. *Geophys. Res. Lett.*, 28:1391–139.
- Mertens, C. J. and et al. (2004). SABER observations of mesospheric temperatures and comparisons with falling sphere measurements taken during the 2002 summer MaCWAVE campaign. *Geophys. Res. Lett.*, 31:L03105, doi:10.1029/2003GL018605.
- Mlynczak, M. G. (1997). Energetics of the mesosphere and lower thermosphere and the SABER Experiment. *Adv. Space Res.*, 20(6):1177–1183, doi:10.1016/S0273-1177(97)00769-2.
- Oberheide, J., Hagan, M. E., and Roble, R. G. (2003). Tidal signatures and aliasing in temperature data from slowly precessing satellites. *J. Geophys. Res.*, 108(A2), doi:10.1029/2002JA009585.

- Pancheva, D., Mukhtarov, P., Andonov, B., Mitchell, N. J., and Forbes, J. M. (2009a). Planetary waves observed by TIMED/SABER in coupling the stratosphere-mesosphere-lower thermosphere during the winter of 2003/2004: Part 1 - Comparison with the UKMO temperature. *J. Atmos. Solar-Terr. Phys.*, 71:61–74, doi:10.1016/j.jastp.2008.09.016.
- Pancheva, D., Mukhtarov, P., Andonov, B., Mitchell, N. J., and Forbes, J. M. (2009b). Planetary waves observed by TIMED/SABER in coupling the stratosphere-mesosphere-lower thermosphere during the winter of 2003/2004: Part 2 - Altitude and latitude planetary wave structure. *J. Atmos. Solar-Terr. Phys.*, 71:75–87, doi:10.1016/j.jastp.2008.09.027.
- Pogoreltsev, A. I., Vlasov, A. A., Fröhlich, K., and Jacobi, C. (2007). Planetary waves in coupling the lower and upper atmosphere. *J. Atmos. Solar-Terr. Phys.*, 69:2083–2101.
- Richards, P. G., Fennelly, J. A., and Torr, D. G. (1994). EUVAC: A Solar EUV Flux Model for Aeronomic Calculations. *J. Geophys. Res.*, 99(A5):8981–8992, doi:10.1029/94JA00518.
- Strobel, D. F. (1978). Parameterization of the atmospheric heating rate from 15 to 120 km due to  $O_2$  and  $O_3$  absorption of solar radiation. *J. Geophys. Res.*, 83:6225–6230.
- Swinbank, R. and Ortland, D. A. (2003). Compilation of the wind data for the Upper Atmosphere Research Satellite (UARS) Reference Atmosphere Project. *J. Geophys. Res.*, 108(D19):4615.
- Zhang, X., Forbes, J. M., Hagan, M. E., Russell III, J. M., Palo, S. E., Mertens, C. J., and Mlynczak, M. G. (2006). Monthly tidal temperatures 20-120 km from TIMED/SABER. *J. Geophys. Res.*, 111:A10S08, doi:10.1029/2005JA011504.

### Addresses of the Authors:

Peter Hoffmann (phoffmann@uni-leipzig.de)  
Christoph Jacobi (jacobi@uni-leipzig.de)

Institute for Meteorology  
University of Leipzig  
Stephanstr. 3  
04103 Leipzig